ISIJ International, Vol. 48 (2008), No. 4, pp. 483–488

Metallurgical and Mechanical Properties of Fusion Zones of TRIP Steels in Laser Welding

Mingsheng XIA,[1,2)] Zhilin TIAN,[2)] Lin ZHAO[2)] and Y. Norman ZHOU[1)]

1) Centre for Advanced Materials Joining, University of Waterloo, Waterloo, Ontario, Canada.
E-mail: mingshengxia@yahoo.ca 2) Central Iron & Steel Research Institute, Beijing, China.

(*Received on September 3, 2007; accepted on January 14, 2008*)

Transformation induced plasticity (TRIP) steels are a promising solution for the production of cars with low body mass because of the combination of high strength and high plastic strain capacity that they offer. Si and Al are two important alternatives for alloying of TRIP steels in order to suppress carbide precipitation in the bainite holding temperature range during steel manufacture. Weldability of TRIP steel is one of the key factors governing its application in auto industry. In this paper, Al-alloyed TRIP steel was investigated with the diode laser welding process in terms of fusion zone metallurgical and mechanical properties, with Si-alloyed TRIP steel also included for comparison. It was found that the fusion zone of the Al-alloyed steel has a multiphase microstructure, containing skeletal ferrite, bainitic ferrite, martensite and retained austenite of two different morphologies. In contrast, the Si-alloyed steel fusion zone consists almost entirely of martensite. The high martensite content results in low fusion zone ductility in the Si-alloyed steel, only providing half the tensile elongation of the Al-alloyed steel. The Si-alloyed steel shows a greater decrease of the strength–ductility balance (ultimate tensile strength times elongation) due to welding, *i.e.*, 62.9 % compared to 45.2 % for the Al-alloyed steel in quasi-static tensile testing. High strain rate tensile testing with a Hopkinson Bar apparatus shows no significant effect of strain rate on the fusion zone ductility for either steel. The fusion zone of the Al-alloyed steel does not exhibit a detectable TRIP effect probably due to the low carbon content in the retained austenite. Al and Si are both relevant as agents to suppress cementite precipitation, but they are found to exert very different influences on steel weldability.

KEY WORDS: metallurgical and mechanical properties; fusion zone; TRIP steel; laser welding.

1. Introduction

The use of high strength steels has increased in the automotive industry in order to reduce automotive body weight. In general, increase of steel strength leads to reduction in tensile elongation and overall plastic strain capacity, and considerable research efforts are continuing to develop steel grades with both a high strength and a high elongation. Transformation induced plasticity (TRIP) steel is a promising solution to achieve a better combination of formability and strength than conventional steels.[1)] The microstructure of these steels typically consists of polygonal ferrite, bainite, martensite, and retained austenite (~10–20 %). The main phenomenon responsible for the improved mechanical properties has been proposed to be the deformation-induced transformation of the metastable retained austenite to martensite during straining.[1)]

The standard CMnSi TRIP steel contains typically about 0.15 wt% carbon, 1.0–2.5 wt% silicon and 1.0–3.0 wt% manganese. Silicon is added to suppress cementite formation during the bainite holding temperature thus forcing more carbon into the retained austenite. However, this steel composition forms a very stable Mn_2SiO_4 oxide film on the surface during the annealing process. The surface tension properties of this oxide, when in contact with liquid Zn, inhibit the galvanizability[2)] and as a result the TRIP steels are currently generally electrogalvanized rather than hot dip galvanized. Alternative alloy elements could be considered. Possible candidates to substitute for Si are Al, P and Cu, which are known to play a similar role as Si.[3–7)] According to Meyer,[8)] the partial replacement of Si by Al in TRIP steels results in a much improved galvanizability. Maki also conducted research on the galvanizability of Si-free CMnAl and Al-free CMnSi TRIP steels respectively and similar results were obtained.[9)] Furthermore, the mechanical properties of cold rolled Si free CMnAl TRIP steel were comparable to those of conventional CMnSi TRIP steels.[10)] The Al-bearing TRIP steel was found to exhibit a remarkable TRIP effect during tensile testing, comparable to Si-containing grades.[7)]

In welding research, some studies have been conducted on Si-alloyed TRIP steels with the laser welding process.[11–13)] However, there is a lack of published weldability studies of Al-alloyed TRIP steels. In this work, the fusion zone metallurgical and mechanical properties of Si- and Al-TRIP sheet steels welded with a diode laser are reported. The detailed solidification behavior and microstructure evolution in Al-TRIP steel fusion zones are documented elsewhere.[14)]

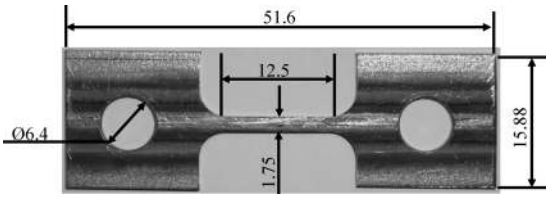

Fig. 1. Dimension (mm) for tensile specimen.

2. Experimental Procedures

Two TRIP steels, alloyed with Al and Si respectively, were autogenously welded with a Nuvonyx ISL-4000 diode laser. This 4 kW AlGaAs laser has a wavelength of 805± 5 nm producing a rectangular beam of 12 mm long by 0.9 mm wide at the focal plane. The focal length is 80 mm during welding. The diode laser welding process lies between arc welding and Nd:YAG or CO_2 laser welding in terms of energy density.[15)]

Butt welding was conducted with full penetration (thus ensuring nearly 2D heat flow in the sheet). The welding speeds ranged from 1.2 to 2.2 m/min depending on sheet thickness. Argon was employed as shielding gas, at a flow rate of 30 L/min.

After welding, representative transverse specimens were cut, mounted, polished and etched, then examined by optical microscopy. Transmission electron microscopy (TEM) was also employed to identify fusion zone microstructure. Vickers micro-hardness testing was carried out at a load of 500 g. Fusion zone tensile testing at room temperature was carried out on miniature specimens excluding base metal and HAZ (heat affected zone). A universal Instron tensile machine and a tensile split Hopkinson Bar apparatus were employed to conduct quasi-static and dynamic tensile tests at the strain rates of 10^{-3} and $1.5\times10^{3}\,s^{-1}$ respectively. Reference marks on the gage length made it possible to acquire total elongation after tensile testing. To facilitate comparison, the same specimen size was also applied to base metal tests (**Fig. 1**). Fracture surfaces after tensile testing were observed using scanning electron microscopy (SEM).

3. Results and Discussion

3.1. Base Metal Characterization

As shown in **Fig. 2**, both base metal microstructures are composed of polygonal ferrite (grey), bainite (black) and retained austenite (white). The samples were etched with Lepera's reagent.[16)] The area fraction of retained austenite in the Al-alloyed steel is about 13%, a little bit higher than that in the Si-alloyed steel, about 12%. The major alloying elements are shown in **Table 1**. The carbon equivalent (CE) is evaluated with Yurioka formula as follows[17)]:

$$CE = C + f(C)\{Si/24 + Mn/6 + Cu/15 + Ni/20 + (Cr + Mo + Nb + V)/5\} \quad \ldots\ldots(1)$$

Where $f(C) = 0.75 + 0.25\tanh\{20(C - 0.12)\}$.

3.2. Weld Hardness Distribution

Figure 3 shows the characteristic weld hardness distributions with a welding speed of 1.6 m/min, in which 251 Hv and 221 Hv are the base metal hardness values for Si and Al-alloyed steel respectively. The difference in base metal hardness is believed to result mainly from the chemistry difference even though the steels have similar CE (Table 1) because Si is a very effective solid-solution strengthening element in the ferrite phase.[7)] In the weld fusion zone, the hardness of the Si-alloyed steel is far above that of the Al-alloyed steel. As discussed later, this is due to fundamental differences in weld microstructure between the steels. Outside the fusion zone, hardness decreases gradually to the base metal level. Soft zones are also observed in the outer HAZ, discussion of which is beyond the scope of this paper.

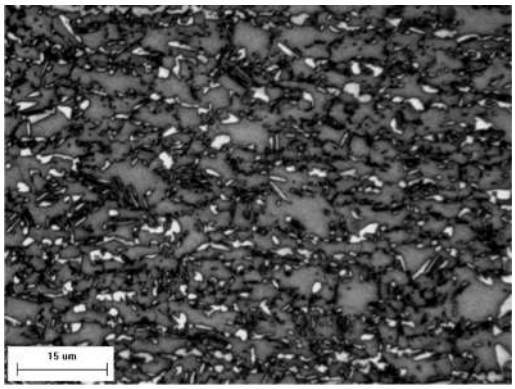

(a) Si-alloyed

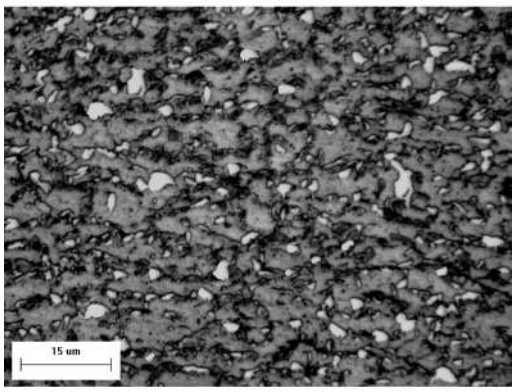

(b) Al-alloyed

Fig. 2. Base metal microstructure.

Table 1. Major contents of experimental steels (wt%).

Grade (thickness in mm)	C	Mn	Al	Si	CE
Si-alloyed (1.2)	0.19	1.63	0.04	1.62	0.53
Al-alloyed (1.1)	0.15	2.13	1.73	0.09	0.47

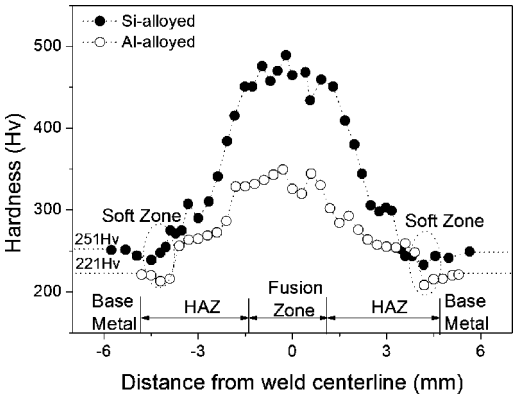

Fig. 3. Weld hardness profiles for two steels with welding speed of 1.6 m/min.

Table 2. Fusion zone hardness at all welding speed (m/min).

Welding speed	1.2	1.4	1.6	1.8	2.0	2.2
Al-alloyed			331±4	334±4	349±3	346±4
Si-alloyed	471±6	465±5	484±5	484±5	494±3	

The effect of welding speed on fusion zone hardness is shown in **Table 2**. It is known that with the diode laser welding process under 2D heat flow, the increase of welding speed will result in a slight increase in cooling rate which leads to corresponding increase of fusion zone hardness. But it can be expected that the overall makeup of the fusion zone microstructures will vary little within the range of welding speeds used. Therefore, the following results concentrate on data from a welding speed of 1.6 m/min.

3.3. Microstructural Characteristics

The large fusion zone hardness disparity between two steels is attributed to their significant difference in microstructure (**Fig. 4**). With cooling rate being very similar among the welds examined, the difference in metallurgical response is evidently dominated by chemistry. Etching with Lepera's reagent[16] reveals that the fusion zone of the Si-alloyed steel is comprised essentially entirely of a single phase of martensitic morphology, Fig. 4(a). The measured fusion zone hardness (484 Hv) is even higher than the martensite hardness (460 Hv) calculated with the Yurioka formula as follows.[18]

$$H_M = 884C + 294 \quad \text{.....(2)}$$

Where C is the carbon content (wt%).

This comparison confirms that the fusion zone microstructure of the Si-alloyed steel is essentially martensite. The high content of Si and Mn is believed to push the experimental fusion zone hardness to a higher level since elements such as C and N will remain constant when welding with high purity Ar shield.

In contrast, the Al-alloyed steel fusion zone comprises a multiphase microstructure as shown in Fig. 4(b) and as a result the experimental fusion zone hardness (331 Hv) is well below the calculated value (427 Hv using Eq. (2)) for a fully martensitic structure. This sample was etched with nital followed by Lepera's reagent to improve the contrast between ferrite and other phases. A significant amount of skeletal ferrite (about 30% in area fraction) is found in the fusion zone. Apart from difference in carbon content between the two investigated steels, the choice of Si or Al as an agent for delaying carbide precipitation appears to play a decisive role in the development of their microstructures. It is well known that Al is a strong ferrite stabilizer and promotes high temperature ferrite as the primary phase in the solidification process.[19] For example, in welds made by striking an arc on a stationary steel cylinder with the chemistry of Fe–0.23C–0.56Mn–0.26Si–1.77Al, ferrite with skeletal morphology at room temperature has also been found with the solidification cooling rate as high as 10^3 K/s.[19] This type of skeletal ferrite has been previously identified[14] as a remnant of high temperature delta ferrite that did not fully transform to austenite during cooling. Furthermore, some evidence was seen in the transformed microstructure in between the skeletal ferrite, of fine ferrite sideplates alongside bainite/martensite. This difference in austenite decomposition products between the fusion zones of the two steels can be partially explained by examination of CCT behaviour. **Figure 5** shows published CCT data for two TRIP steels with the chemistries of Fe–0.2C–1.49Mn–2.03Si and Fe–0.2C–1.47Mn–2.18Al respectively. This comparison indicates that Al has a greater propensity than Si for generating ferrite and bainite during transformation from austenite in continuous cooling.[20]

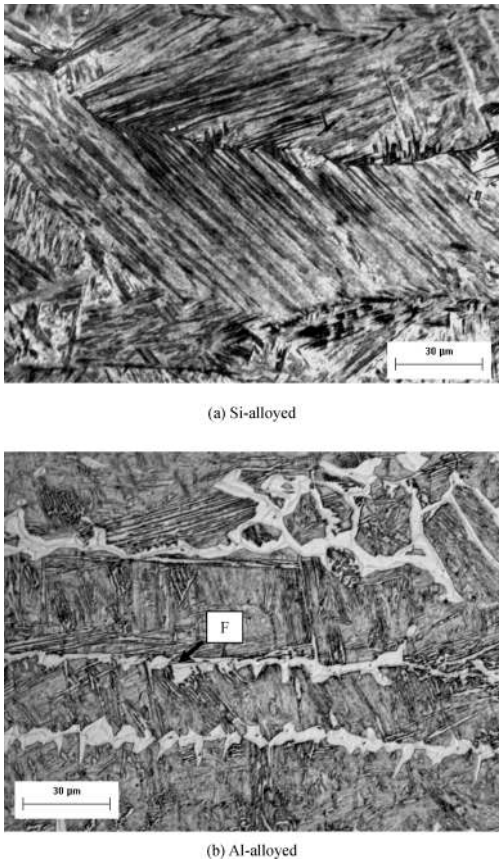

Fig. 4. Optical fusion zone microstructure.

In TEM observation of welds in the Al-alloyed steel, two kinds of retained austenite were observed in the fusion zone, shown in **Fig. 6** respectively. One was austenite films between bainitic ferrite laths, Fig. 6(a). The bainite covers about 65% area percentage of the fusion zone, as determined in previous research.[14] The other morphology was chunk shaped austenite occasionally observed dispersed in the ferrite matrix, Fig. 6(b). The retained austenite can be attributed to the role played by the Al in suppressing the carbide precipitation.[6] Also the presence of retained austenite is expected to enable the fusion zone have the TRIP effect by transforming to martensite on straining and contributes to uniform elongation, which is desired in TRIP steel welding in order to achieve matching properties with base metal.

3.4. Mechanical Properties

3.4.1. Tensile Testing Behaviour

The results of tensile tests of base metal and weld fusion zone coupons are summarized in **Table 3**, including ultimate tensile strength (*TS*) and total elongation (*EL*). Each datum is an average of results from three coupon tests. It is found that the base metal tensile strengths in dynamic ten-

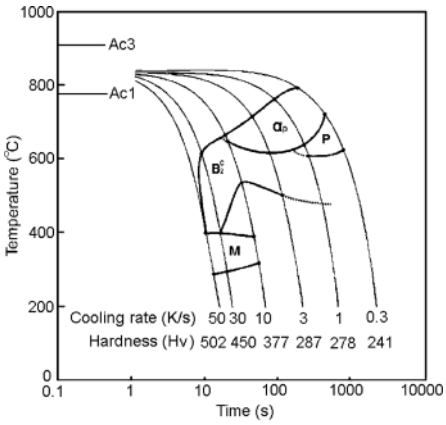

(a) Si-alloyed steel

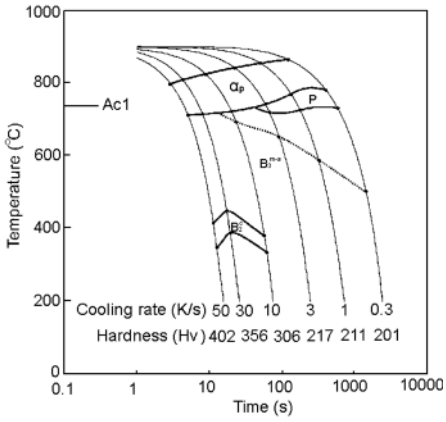

(b) Al-alloyed steel

Fig. 5. CCT diagrams of two TRIP steels.[20]

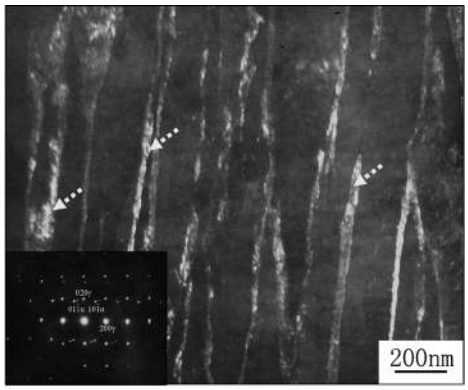

(a) Filmy RA between lathy bainitic ferrite

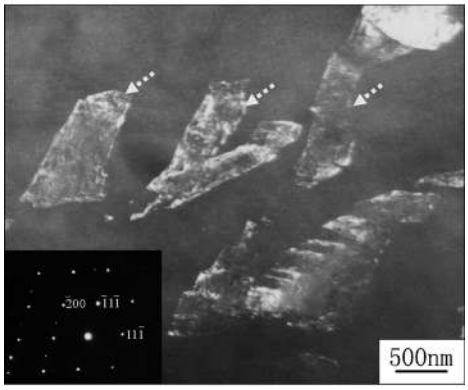

(b) Chunk shaped RA dispersed in ferrite matrix

Fig. 6. TEM dark field images showing the retained austenite (white) in Al-alloyed TRIP steel.

Table 3. Tensile properties of experimental steels (welding speed: 1.6 m/min).

	Strain rate (s^{-1})	Si-alloyed		Al-alloyed	
		σ (MPa)	e (%)	σ (MPa)	e (%)
Base metal	10^{-3}	836±8	27.1±0.6	743±2	23.8±0.3
	1.5×10^{3}	1182±39	24.0±0.2	1089±5	20.1±0.2
Fusion zone	10^{-3}	1545±14	5.6±0.5	1080±6	9.0±0.5
	1.5×10^{3}	1912±39	5.5±0.3	1391±24	8.7±0.7

sile testing are higher than those conducted at quasi-static testing conditions. This is a frequently observed finding in testing of automotive steels, and the usually understood reasons are that during deformation at high strain rates, additional multiplication of dislocations occurs around hard phases and less time is available for accommodation processes, which effects make dislocation sliding more difficult and lead to effective strengthening of the ferrite matrix. At the same time, the elongation exhibits a decrease since the progressive transformation of retained austenite into martensite is suppressed at high strain rates.[21] The changes of strength and elongation for these TRIP steels according to strain rates are consistent with previously reported work.[22] However, the Si-alloyed base metal possesses higher strength and ductility than the Al-TRIP steel for the following reasons. First, the selection of Si as a functional alloying element is known to greatly improve ferrite matrix strength, compared to use of Al.[7] Second, the higher total elongation of the Si-alloyed steel is expected to be related to retained austenite stability, as determined by carbon content and by morphology and size of the austenite grains, and the morphologies of other microstructural constituents.[23] Among all these factors the most important factor is the carbon content of austenite.[24] Between these base metals, the retained austenite volume fraction is higher in the Al-alloyed steel which also contains less carbon than the Si-alloyed steel. By mass balance, the carbon content in the retained austenite of the Al-alloyed steel is lower, which is understood to reduce austenite stability during deformation (*i.e.*, leading to nearly complete transformation to martensite at low strain levels) and a decrease in uniform elongation.[25,26]

In the case of the Si-alloyed steel fusion zone, the finding of very little change in ductility with strain rate is not surprising and apparently due to its entirely martensitic microstructure. For the Al-alloyed steel, the fusion zone also shows little elongation variation in spite of the presence of retained austenite. According to previous research,[27,28] retained austenite as films between the subunits of bainitic ferrites and as chunks can both contribute to the TRIP effect by transforming under strain. A key parameter for the effect of transformation on ductility is the stability of the austenite, which is mainly determined by the austenite particle size and composition, especially the carbon content.[24,29] As discussed in relation to the base metal testing, it has been suggested that high strain rate testing can restrict the progressive transformation of retained austenite to martensite and as a result, the contribution from the strain-induced transformation to uniform elongation or total elongation may be less than that in quasi-static testing.[21] So it could be expected that there should be effects of elongation on strain rate for steels with notable TRIP effect as is found in these base metals. The underlying reason for the relative

lack of strain rate effect on ductility in this Al-alloyed weld metal is probably related to the formation of retained austenite with low carbon content and resultant very low stability under strain or stress. So the expected martensitic transformation occurs too early under quasi-static testing, and as a result contributes little to the overall ductility at either low or high strain rates. That is to say, the effectiveness of the TRIP phenomenon in this Al-alloyed steel weld metal is too low to be significant.

The fusion zone strength of the Si-alloyed steel exhibits a higher increase compared to its base metal than that of Al-alloyed steel due to the fundamental difference in microstructure. But the latter enjoys better retention of ductility. SEM observation of the fracture surfaces after tensile testing at the strain rate of $10^{-3}\,s^{-1}$ shows markedly different characteristics between them. The Al-alloyed fusion zone exhibits a mixed fracture surface with dimples and cleavage while the Si-alloyed weld metal shows essentially all cleavage fracture, shown in **Fig. 7**.

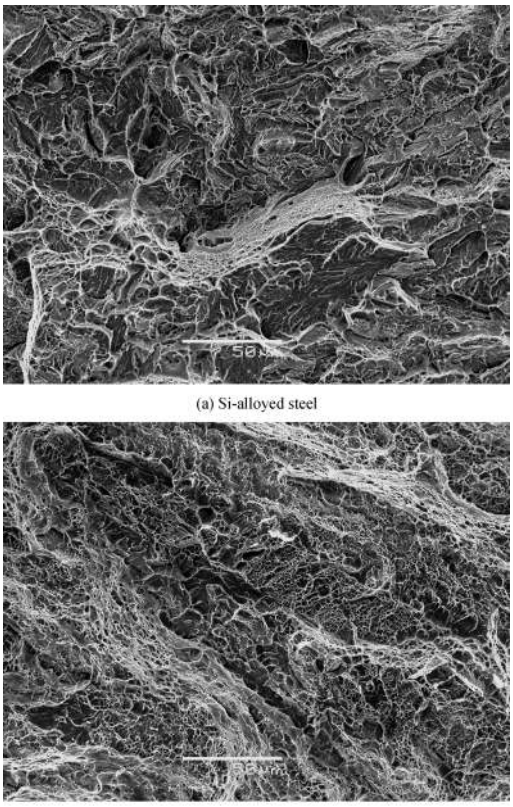

(a) Si-alloyed steel

(b) Al-alloyed steel

Fig. 7. Fusion zone fractography of tensile test coupons at the engineering strain rate of $10^{-3}\,s^{-1}$.

3.4.2. Strength–Ductility Balance

Often the product of tensile strength and total elongation is used as a measure to evaluate the stretch formability of steels.[30] The data calculated from tensile testing are shown in **Fig. 8** for both steels. It is found that the Si-alloyed base metal shows a better combination of strength and total elongation than that of the Al-alloyed steel at corresponding strain rates. The difference was explained above. After welding, fusion zones for both steels show a marked decrease of strength–ductility balance. This means the welding process has a detrimental influence on the steels' formability behavior. But the Al-alloyed fusion zone has a lower decrease (45.1%) than that of the Si-alloyed steel (62.9%) at the quasi-static strain rate. The decrease is also similar for the dynamic tensile tests, although strain rate-induced increases in strength lead to higher strength–ductility balances.

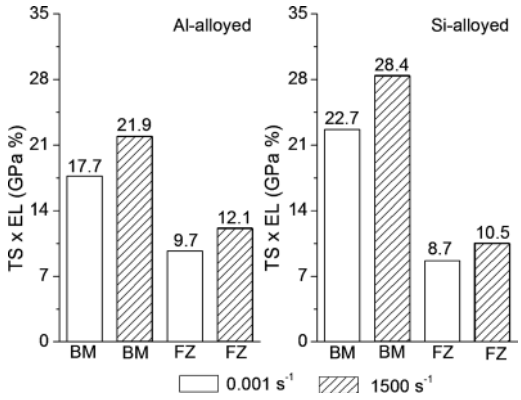

Fig. 8. Strength ductility balance of base metal (BM) and fusion zone (FZ).

4. Conclusions

Two TRIP steels alloyed with Al or Si were butt welded with a diode laser and the fusion zones were characterized in terms of metallurgical and mechanical properties. Conclusions are as follows:

(1) The Al-alloyed steel has lower hardening capacity than the Si-alloyed steel. Different microstructural constituents are seen in the fusion zone of the respective steels. The Si-alloyed fusion zone is predominantly composed of martensite while the Al-alloyed steel fusion zone shows a multiphase microstructure, containing skeletal ferrite, bainitic ferrite, martensite and retained austenite with two kinds of morphology. The difference in microstructure mainly results from the use of different alloying element choices, specifically Si and Al, which have very different influences in terms of austenite stability.

(2) The Si-alloyed TRIP base metal possesses a better combination of strength and elongation than that of the Al-alloyed TRIP steel. But after welding, the Si-alloyed steel fusion zone shows a higher decrease of strength–ductility balance than that of the Al-alloyed steel in both quasi-static and dynamic tensile tests.

(3) The fusion zone ductility is not sensitive to strain rate for either steel. The Al-alloyed steel fusion zone with the presence of retained austenite does not exhibit a detectable strain rate TRIP effect probably due to its low carbon content.

Acknowledgement

The authors appreciate the assistance from technologist Tom Gawel and Dr. Christopher Salisbury from the formability group at the University of Waterloo for conducting the high strain rate tensile tests and for related discussion. This work was supported financially by Auto21 (www.auto21.ca), Dofasco, Huys Industries Ltd., Centerline Ltd., and International Lead Zinc Research Organization (USA).

REFERENCES

1) V. F. Zackay, E. R. Parker and R. Busch: *Trans. ASM*, **60** (1967), 252.
2) M. Isobe, C. Kato and K. Mochizuki: Proc. 39th Conf. on Mechanical Working and Steel Processing, ISS, Warrendale, PA, (1997), 121.
3) H. C. Chen, H. Era and M. Shimizu: *Metall. Trans. A*, **20A** (1989), 437.
4) B. Liesbeth, V. Kim and E. Wettinck: *ISIJ Int.*, **46** (2006), 1251.
5) A. Pichler and P. Stiazny: *Steel Res.*, **70** (1999), 459.
6) M. D. Meyer, D. Vanderschueren and B. C. De. Cooman: *ISIJ Int.*, **39** (1999), 813.
7) E. Giraulta, A. Mertensb, P. Jacquesb, Y. Houbaertc, B. Verlindena and J. V. Humbeecka: *Scr. Mater.*, **44** (2001), 885.
8) J. Mahieu, S. Claessens, M. D. Meyer and B. C. De. Cooman: Proc. on Galvanised Steel Sheet Forum—Automotive, The Institute of Materials, London, UK, (2000), 185.
9) J. Maki, J. Mahieu, B. C. De. Cooman and S. Claessens: *Mater. Sci. Technol.*, **19** (2003), 125.
10) J. Maki, J. Mahieu and B. C. De. Cooman: Proc. 5th Int. Conf. on Zinc and Zinc Alloy Coated Steel Sheet (Galvatech 2001), Centre de Researches Meâtallurgiques, Bruxelles, Belgium, (2001).
11) T. K. Han, S. S. Park, K. H. Kim, C. Y. Kang, I. S. Woo and J. B. Lee: *ISIJ Int.*, **45** (2005), 60.
12) J. L. Bocos, F. Zubiri, F. Garciandia, J. Pena, A. Cortiella, J. M. Berrueta and F. Zapirain: *Weld. Int.*, **19** (2005), 539.
13) S. Daneshpour, S. Riekehr, M. Koçak, V. Ventzke and A. I. Koruk: *Sci. Technol. Weld. Joining*, **12** (2007), 508.
14) M. Xia, Z. Tian, L. Zhao and Y. Zhou: *Mater. Trans.*, **49** (2008).
15) L. Li: *Opt. Lasers Eng.*, **34** (2004), 231.
16) F. S. LePera: *J. Met.*, **32** (1980), 38.
17) N. Yurioka and T. Kasuya: *Weld. World*, **35** (1995), 327.
18) N. Yurioka: IIW Doc IX-2058-3, (2003).
19) S. S. Babu, J. W. Elmer, S. A. David and M. A. Quintana: *Proc. R. Soc. (London)*, **458** (2002), 811.
20) P. A. Manohar, K. Kunishige, T. Chandra and M. Ferry: *Mater. Sci. Technol.*, **118** (2002), 856.
21) W. Bleck, P. Larour and A. Bäumer: *Mater. Sci. Forum*, **29** (2005), 21.
22) X. C. Wei, R. Y. Fu and L. Li: *Mater. Sci. Eng. A*, **A465** (2007), 260.
23) L. Samek, B. C. De. Cooman, J. V. Slycken, P. Verleysen and J. Degrieck: Proc. of Int. Symp. on Transformation and Deformation Mechanism in Advanced High-Strength Steels, ed. by M. Militzer, W. J. Poole and E. Essadiqi, CIM, Montreal, (2003), 77.
24) K. Sugimoto, A. Nagasaka, M. Kobayashi and S. Hashimoto: *ISIJ Int.*, **39** (1999), 56.
25) M. Mukherjee, O. N. Mohanty, S. Hashimoto, T. Hojo and K. Sugimoto: *ISIJ Int.*, **46** (2006), 316.
26) M. L. Brandt and G. B. Olson: *Iron Steelmaker*, **20** (1993), 55.
27) M. Takahashi and B. K. D. H. Bhadeshia: *Mater. Trans., JIM*, **32** (1991), 689.
28) I. B. Timokhina, P. D. Hogson and E. V. Pereloma: *Metal. Mater. Trans. A*, **35A** (2004), 2331.
29) P. J. Jacques, J. Ladriere and F. Delannay: *Metall. Mater. Trans. A*, **32A** (2001), 2759.
30) K. Sugimoto, B. Yu, Y. Mukai and S. Ikeda: *ISIJ Int.*, **45** (2005), 1194.